DOI: 10.21062/mft.2023.018 http://www.journalmt.com

Influence of Structural State prior Quenching in Spring Steel

Jakub Kotous (0000-0001-9141-8477)[1], Pavel Salvetr (0000-0001-5717-267X)[1], Daniela Nacházelová (0000-0002-0050-6859)[1]
[1]COMTES FHT a.s., Prumyslova 995, 334 41 Dobrany. Czech Republic.
E-mail: jkotous@comtesfht.cz, psalvetr@comtesfht.cz, dnachazelova@comtesfht.cz.

Various structure states before quenching significantly influence final mechanical properties as well as the dispersion of chemical composition at the same steel grade. Therefore heat treatment with mechanical properties is specified in the technical delivery conditions. Even if the heat treatment is determined, different mechanical properties can be achieved. These differences are increasing in importance in high-strength applications like springs, cutting tools, safety, and load-bearing parts of automotive design ect. Because it has a direct impact on their lifetime. The structure consists of ferrite and cementite after spheroidization annealing prior quenching process. The cementite could be observed in various shapes, e.g. fine and large globular particles or the rest of the disintegrated lamellar shape. This article shows how these cementite morphologies affect the quenching behavior and final mechanical properties in high-strength spring steel 54SiCr6.

Keywords: Accelerated Spheroidization, ASR, Quenching, Spring steel, 54SiCr6.

1 Introduction

The mechanical properties of heat-treated steel are typically determined by quenching and tempering processes. These as well as entire technological procedures are verified and often not changed. Effort not to interfere with the processing settings results from higher knowledge requirements for the operators. Then deviation of resultant properties is based on the technical delivery conditions i.e. the supplier and his material. The delivery conditions of high-strength steels are usually soft annealed state. This requirement can be defined by metallography (carbide spheroidization analysis) or mostly hardness measurement by maximal value. It leads to a big range in terms of structural conditions and possible trouble for following heat treatments in high-strength applications [1–5].

The processing to achieve these requirements are many e.g. procedures of soft annealing are many. The classical soft annealing is performed around temperature A_1. During annealing, the cementite lamellas are spheroidized creating round cementite particles in the ferritic matrix. This convention annealing is a rather time-consuming diffusion process and the processing time takes normally tens of hours. After the spheroidizing process, the material is slow cools down especially important when annealing is performed above A_1 [6–8]. Moreover, carbide spheroidization is retarded in steels with higher Si due to worsened diffusion of carbon [9, 10].

Nowadays there are many ways to achieve soft annealed structure and acceleration during treatment. There is various combination of heating above and then under A_1, thermal cycling around A_1, overheating with undercooling… All this furnace treatment takes from tens to units of hours [7, 11, 12]. The effectively accelerating can be reached by a more drastic change in technology. Induction heating allows using a fast heating process while new utilization of divorced eutectoid transformation (DET) [12–14]. Spheroidization based on the cycling of fast induction heating with DET effect is a key part of technology "Accelerated Spheroidization and Refinement". This ASR process leads to a spheroidized structure in minutes [15, 16]. The other way to rapidly accelerated spheroidization ASR is based on thermomechanical treatment [17].

The advanced processing influences the size of globular carbides as well as the size of an original austenitic grain. This trend causes slowing down the decrease in hardness because rising influence of strengthening of dispersion and from smaller OAG [18]. Generally, a shorter processing time leads to finer carbides and austenitic grain if the process is well set. If not shorter processing time is at the expense of lesser degrees of spheroidized carbide particles. The number of lamellar carbides rise the hardness of annealed material [19]. Hardness criterium can become misleading from point of view of advanced spheroidization [20]. A reliable solution is a metallographic analysis that should always be in the case of high-strength materials.

The main goal of this work was to achieve different pearlitic structures in high-strength spring steel 54SiCr6 and their comparison in point of view

austenitization behavior and resultant mechanical properties. The structures before quenching were achieved by soft annealing, Accelerated Spheroidization and Refinement (ASR) process, and air cooling after hot rolling. Microstructure evolution was observed by scanning electron microscopy. Basic mechanical properties were determined by hardness measurement and tensile tests.

The 54SiCr6 steel is used in high stressed shape springs and high-strength wires. It is commonly processed to 1500-2000 MPa in ultimate strength with min. 6 % elongation and reduction of area of more than 25 % for shape spring parts. The modern trend is achieved strengths over 2000 MPa maintaining good toughness. Especially in the spring wire industry where the area reduction requirement is min. 35 %. This is precisely why ensuring a suitable fine structure is the first step in the optimization of processing.

2 Materials and methods

The experimental material under investigation was 54SiCr6 spring steel. The chemical composition is given in Tab. 1 (measured with Q4 TASMAN optical emission spectrometer). The experimental steel was prepared by vacuum induction melting, the ingot was heated up to 1100 °C and subsequently forged to block 90x250 mm, then hot rolled to 24 mm thick plates and air cooled. Cylindrical samples 20 mm in diameter and 130 mm in length were machined.

Tab. 1 *Chemical composition of experimental steel and 54SiCr6 standard according to ČSN EN 10089 in wt. %*

Steel	C	Si	Mn	Cr	P	S	Fe
Exp. batch	0.57	1.51	0.68	0.75	0.008	0.003	bal.
54SiCr6	0.51-0.59	1.20-1.60	0.50-0.80	0.50-0.80	<0.025	<0.025	bal.

First, conventional soft annealing was carried out in an electrical air furnace. The material was held just above the A_{c1} temperature. The soft annealing sequence consisted of heating 60 °C/h to 720 °C, heating 15 °C/h to 770 °C, soaking at 770 °C for 5 hours, slow cooling down at 5 °C/h to 720 °C, cooling at 25 °C/h to 650 °C, free cooling in the furnace to 400 °C and afterward cooling in still air to ambient temperature. The processing duration was 27 hours, till the samples were removed from the furnace.

Second, advanced spheroidization annealing „Accelerated Spheroidization and Refinement“ ASR was performed by medium-frequency induction heating equipment. The ASR process was controlled using a PLC programming unit. The sample temperature was measured with a thermocouple welded onto the surface of heated samples. The ASR sequence consisted of three thermal cycles (Fig. 1). The 1st and the 2nd cycle consisted of fast induction heating at 19 °C/s to 820 °C, soaking at 820 °C for 15 seconds, free cooling to 725 °C, soaking at 725 °C for 300 seconds. The soaking time at 725 °C was extended to 600 seconds in the 3rd cycle. Then samples were cooled down to ambient temperature. The total duration of the accelerated spheroidization ASR till free cooling was approximately 30 minutes.

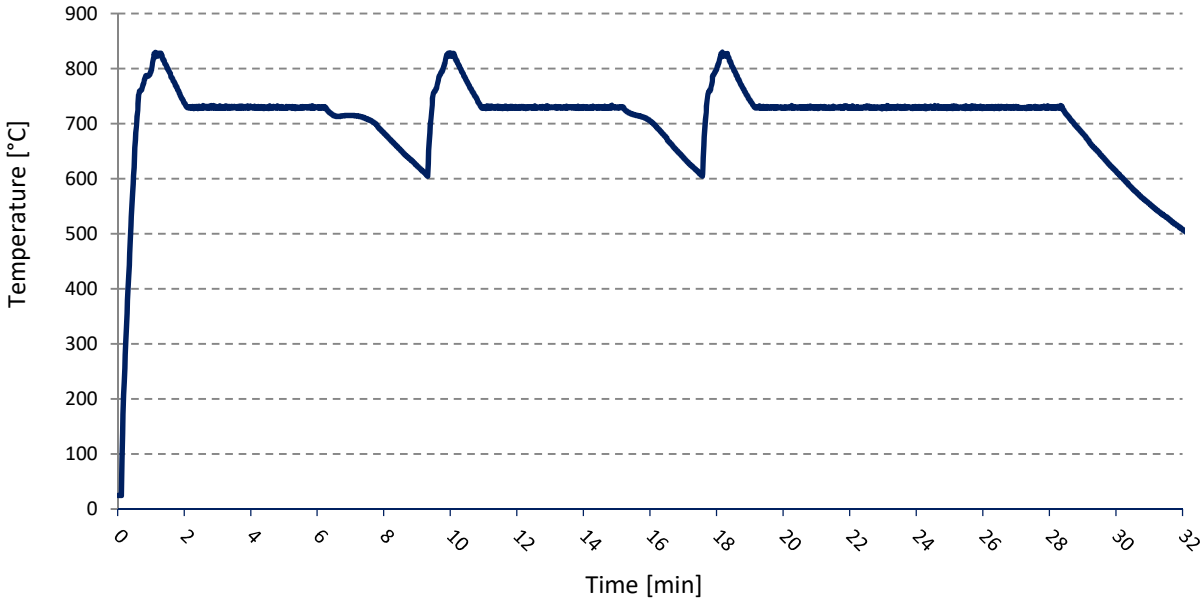

Fig. 1 *Sequence of ASR processing*

Heating for quenching and tempering was carried out using an electrical air furnace. Samples were heated to the austenitization temperature at 810, 830, 850, 870, 890 °C, and 910 °C for 20 or 40 minutes and oil-quenched. All samples were tempered at 400 °C for 2 hours, followed by air cooling.

The samples for microstructure observations were polished, with the final step using colloidal silica with a particle size of 0.05 μm. The microstructure was revealed by etching in a Nital reagent (98 mL of ethanol + 2 mL nitric acid). Next, the microstructure was observed by scanning electron microscope (SEM) JEOL IT 500 HR.

Mechanical properties were tested by tensile tests and hardness measurements. Hardness according to Vickers (ČSN EN ISO 6507-1 standard) with a load of 10 kg was measured at 5 points for each sample [21]. Round tensile samples of 60 mm in gauge length and 10 mm in diameter were tested at a rate of 0.75 mm/min on a Zwick Z250 testing machine with a 250 kN capacity according to ČSN EN ISO 6892-1 at ambient temperature [22]. The standard tension deformation characteristics were evaluated: 0.2 % Offset yield strength ($R_{p0.2}$), Ultimate tensile strength (R_m), Total plastic elongation after a fracture (A), and reduction of area (Z). Three tests were conducted for each condition, and the average value was calculated.

3 Results and discussion

3.1 Initial states before quenching

The lamellar pearlite („LP“) after hot rolling with free air cooling consisted of ferrite and cementite in lamellar form, see Fig. 2. The hardness was 290 ± 7 HV10. The structure was homogeneous. The next spheroidized structure was made from this lamellar pearlite. Globular carbides were predominant after both soft annealing and the ASR processing. It was more than 95 % carbides. The soft annealing produced coarse globular pearlite („CGP“). The size of globular particles was up to 2 μm (Fig. 3). The ASR sequence led to fine globular pearlite („FGP“). The ASR microstructure consisted of densely dispersed globular cementite particles no more than 0.5 μm in size (Fig. 4). Naturally, it led to higher hardness after the ASR process than soft annealing, e.g. 224 ± 5 HV10 for FGP and 207 ± 1 HV10 for CGP. Both heat treatments meet the delivery specifications of 54SiCr6 steel annealed to obtain globular cementite.

The results of the tensile test in initial structures are in Tab. 2. Fine globular pearlite had a higher yield and tensile strength with lower elongation in comparison with coarse globular pearlite. Surprisingly, area reduction was better. The initial state with lamellar pearlite had expected lower plastic properties. The ultimate strength was the highest. The yield strength was the same in lamellar and fine globular pearlite.

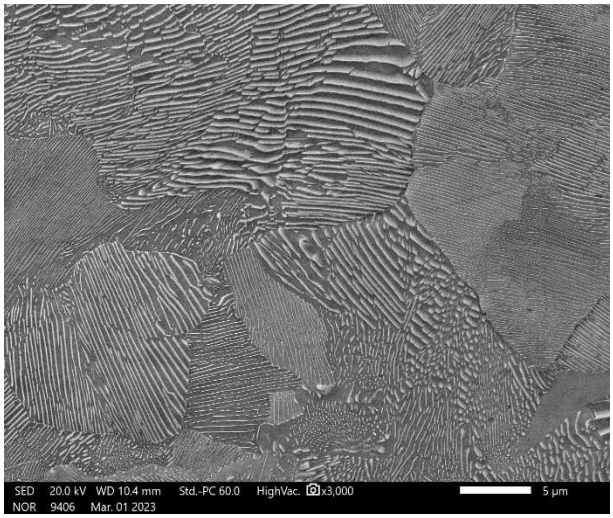

Fig. 2 *Lamellar pearlite after hot rolling, 290 HV10*

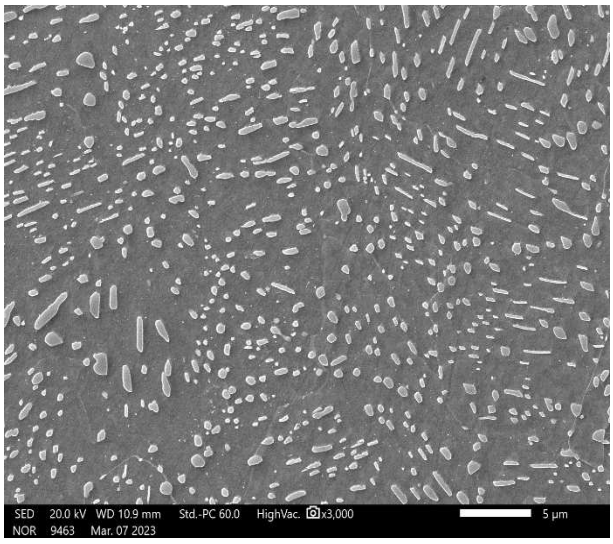

Fig. 3 *Coarse globular pearlite after soft annealing, 207 HV10*

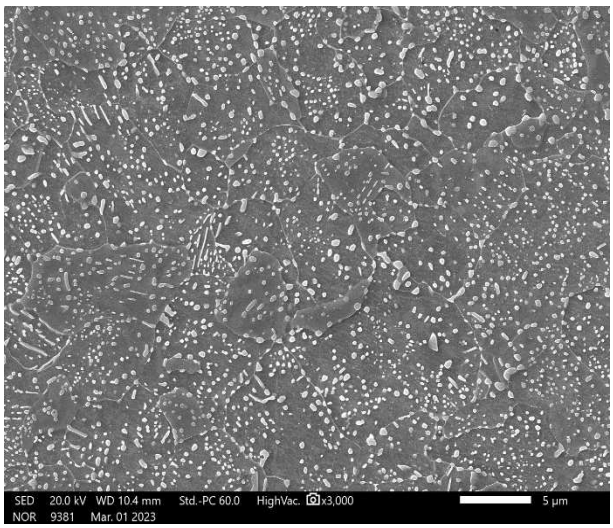

Fig. 4 *Fine globular pearlite after ASR processing, 224 HV10*

Tab. 2 *Mechanical properties of initial states prior to quenching*

Structure	$R_{p0.2}$ [MPa]	R_m [MPa]	A [%]	Z [%]	HV10
Lamellar pearlite („LP“)	542 ± 1	987 ± 2	16.5 ± 0.2	39.0 ± 0.6	290 ± 7
Coarse globular pearlite („CGP“)	356 ± 1	688 ± 2	28.0 ± 0.3	52.5 ± 0.1	207 ± 1
Fine globular pearlite („FGP“)	545 ± 11	803 ± 5	24.0 ± 0.2	63.0 ± 0.1	224 ± 5

3.2 Microstructure after quenching and tempering

All initial states after quenching at the lowest temperature of 810 °C for 20 and 40 minutes contained ferrite. The LP sample included less ferrite compared to CGP and FGP. If the quenching temperature was 830 °C, the LP and FGP samples were acceptably quenched even at 20 minutes of soaking. Both structures are composed of martensite matrix and undissolved carbides, see Fig. 5 and Fig. 6. The austenitization progress in LP and FGP was the same at higher temperatures. Undissolved carbides were very fine globular particles and homogeneously distributed through the matrix. The carbides were fully dissolved at 890 °C for soaking of 20 minutes, respectively 870 °C for 40 minutes of soaking.

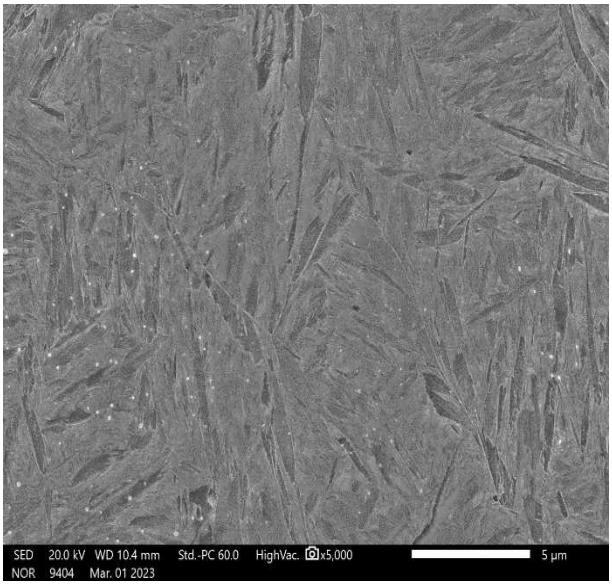

Fig. 5 *Microstructure of LP quenched at 830 °C/ 20 min*

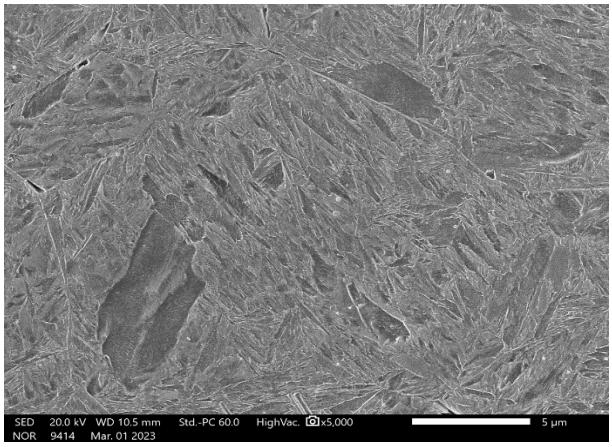

Fig. 6 *Microstructure of FGP quenched at 830 °C/ 20 min*

Quenching CGP made by soft annealing had different progress. Spheroidization and Ostwald´s ripening created coarse carbide particles during long-time soft annealing. Carbon diffusion had a lot of time to cover a relatively large distance and impoverished the ferritic matrix. The sufficient austenitization of ferrite was at a quenching temperature of 870 °C with 20 minutes of soaking which is about 40 °C more than in previous cases. In this case, the twice longer soaking time saved 20 °C. The comparable overview of quenching behavior is in Tab. 3. The difference of 40 °C still lingers on carbide dissolution too. The large undissolved carbides were observed in the quenched CGP structures because the fine one was dissolved at first. Therefore only the big carbides were found at 910 °C with a soaking time of 20 minutes (Fig. 7), and respectively 890 °C for 40 minutes soaking. The full austenitization without undissolved carbides was observed at 910 °C for 40 minutes of soaking. Apparently, the temperature of 930 °C would be successful for full dissolution in 20 minutes of soaking time.

Tab. 3 *Austenitization progress: the highest quenching temperature at which ferrite and carbides were found in the microstructure*

Initial state prior to quenching	**Lamellar pearlite LP**		**Coarse globular pearlite CGP**		**Fine globular pearlite FGP**	
Soaking time [min]	20	40	20	40	20	40
Ferrite	810 °C	810 °C	850 °C	830 °C	810 °C	810 °C
Undissolved carbides	870 °C	850 °C	910 °C	890 °C	870 °C	850 °C

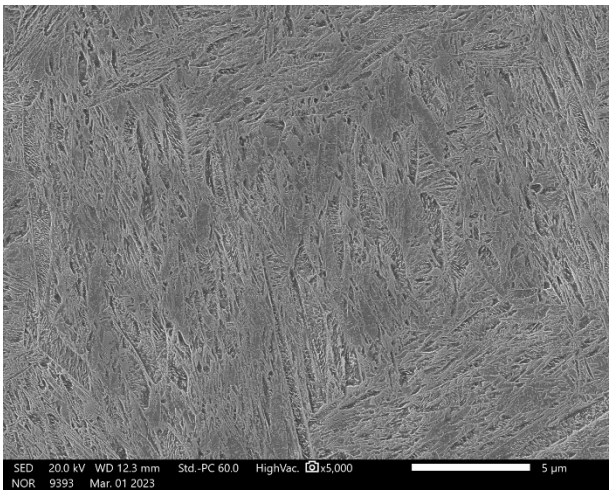

Fig. 7 *Microstructure of CGP quenched at 910 °C/ 20 min*

The difference in martensite among the various initial states prior to quenching was not found in SEM observation. The measuring of the prior austenite grain size was not quantitative because of poor visibility. Etching failed with various methods. The martensitic structure was very fine and no preferential precipitation or segregation along grain boundaries occurred. The prior austenite grain was about the same size after quenched lamellar, coarse, and fine pearlite. It was determined about 12 µm.

Cementite precipitated during tempering at 400 °C. It was located along and within martensite plates. There were found no differences among tempered microstructures obtained in all samples. Only described undissolved carbides, eventually the presence of ferrite caused by quenching.

3.3 Hardness measurement

The results of hardness measurement are in Fig. 8 for 20 minutes of austenitization. It conformed with the microstructure observation. Hardness after full austenitization of ferrite was the same. The dissolution of the remaining carbides did not lead to continuing increase in hardness. This trend was for all initial states the same. All initial conditions had also the same maximum hardness level. The maximum hardness after quenching was about 750 HV10 and roughly 550 HV10 after tempering at 400 °C. The same was valid for a soaking time of 40 minutes during quenching.

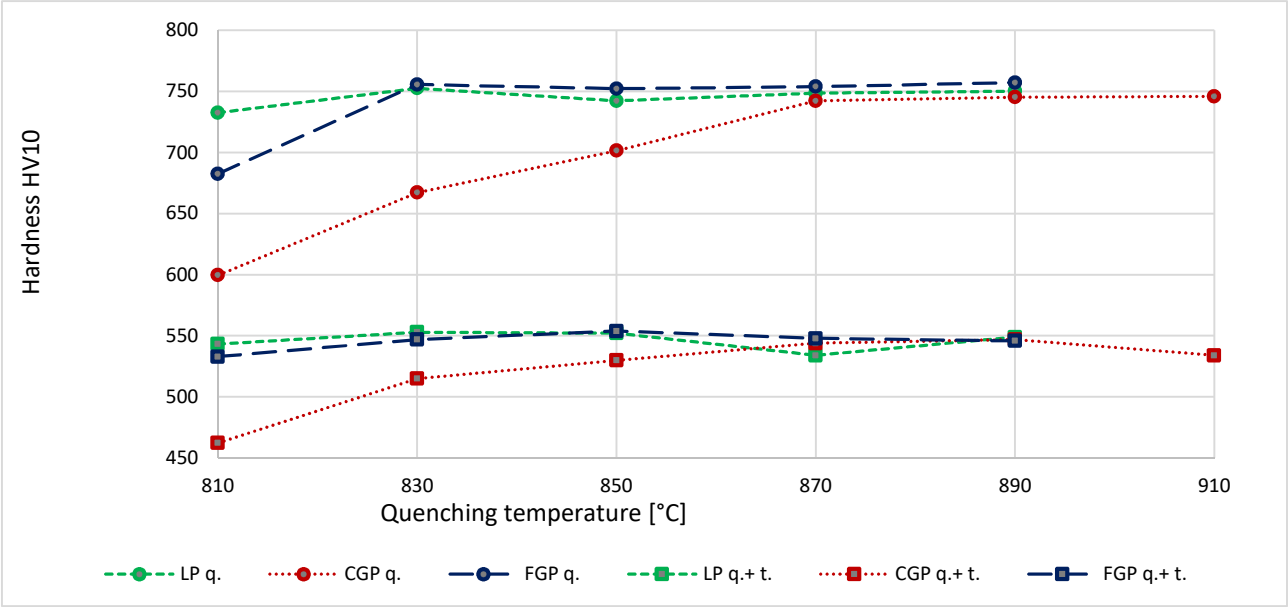

Fig. 8 *Hardness progression of lamellar pearlite (LP), coarse globular pearlite (CGP), fine globular pearlite (FGP) after quenching (q.) and tempering (q.+t.)*

3.4 Tensile test properties after quenching and tempering

The yield and ultimate tensile strengths after hardening of various initial states were not at the same level as the hardness results. The results of tensile testing are in Tab. 4 for austenitization of 20 minutes and in Tab. 5 for austenitization of 40 minutes. Maximum ultimate tensile strength was achieved after quenching of lamellar pearlite. Interestingly, ultimate strength over 1850 MPa could not be exceeded by quenching of coarse globular pearlite with a soaking time of 20 minutes, even at the highest temperature. The ultimate strength of 1881 MPa was obtained at 870 °C and twice longer soaking times. This value was comparable with fine globular or lamellar pearlite.

The highest values of yield strength were achieved in the case of lamellar and fine globular pearlite. Overall, properties were worse in LP with increasing quenching temperature than 830 °C. This could mean that lamellar pearlite was too fast dissolved into austenite and the microstructure began to coarsen during austenitization. In FGP was not observed this trend. The CGP had higher elongation and area reduction than LP. It reached elongation over 9.5 %

in CGP samples and the reduction of area was about 34-35 %. FGP brought better plastic properties. It achieved elongation of over 9.5 % and area contraction of over 40 %. FGP after quenching had high yield and ultimate strength at the same time. In this point of view, FGP had advantages of both lamellar and coarse globular pearlite and in addition a unique improved reduction of area.

Tab. 4 *Summary of mechanical properties, austenitization 20 minutes*

Sequence	$R_{p0.2}$ [MPa]	R_m [MPa]	A [%]	Z [%]	$R_{p0.2}/R_m$ [-]
LP quenched at 830 °C	1720 ± 4	1909 ± 8	9.0 ± 0.3	33.5 ± 1.8	0.90
LP quenched at 850 °C	1667 ± 1	1851 ± 6	8.5 ± 1.1	33.5 ± 0.1	0.90
LP quenched at 870 °C	1666 ± 9	1867 ± 6	8.5 ± 0.8	30.5 ± 0.5	0.89
CGP quenched at 830 °C	1589 ± 5	1765 ± 3	9.0 ± 0.2	32.5 ± 0.1	0.90
CGP quenched at 870 °C	1634 ± 7	1832 ± 12	9.0 ± 0.2	31.5 ± 0.9	0.89
CGP quenched at 890 °C	1656 ± 10	1847 ± 1	9.5 ± 0.2	34.0 ± 1.4	0.90
CGP quenched at 910 °C	1644 ± 18	1835 ± 16	10.0 ± 0.1	35.0 ± 1.0	0.90
FGP quenched at 830 °C	1696 ± 19	1873 ± 13	9.0 ± 0.1	35.0 ± 0.4	0.91
FGP quenched at 850 °C	1686 ± 11	1881 ± 1	9.5 ± 0.1	39.0 ± 0.9	0.90
FGP quenched at 870 °C	1684 ± 19	1863 ± 10	9.5 ± 0.2	41.5 ± 1.1	0.90

*All sequences are tested in quenched and tempered conditions at 400 °C for 2 hours

Tab. 5 *Summary of mechanical properties, austenitization 40 minutes*

Sequence	$R_{p0.2}$ [MPa]	R_m [MPa]	A [%]	Z [%]	$R_{p0.2}/R_m$ [-]
LP quenched at 830 °C	1723 ± 3	1914 ± 7	9.0 ± 0.1	32.5 ± 1.0	0.90
LP quenched at 870 °C	1678 ± 11	1885 ± 3	8.0 ± 0.3	30.0 ± 1.5	0.89
CGP quenched at 830 °C	1660 ± 16	1832 ± 17	8.0 ± 0.5	33.0 ± 0.4	0.91
CGP quenched at 870 °C	1683 ± 7	1881 ± 3	9.0 ± 0.1	34.0 ± 1.0	0.89
FGP quenched at 830 °C	1716 ± 7	1881 ± 11	9.0 ± 0.4	39.0 ± 0.9	0.91
FGP quenched at 870 °C	1694 ± 6	1883 ± 8	9.5 ± 0.4	39.5 ± 0.4	0.90

*All sequences are tested in quenched and tempered conditions at 400 °C for 2 hours

Based on the results, the minimum quenching temperature needs lamellar and fine globular pearlite. The fine globular cementite dissolved almost as quickly as lamellar cementite. The CGP is necessary for austenitization at higher quenching temperatures because austenitizing is retarded. Cementite was present in large globules with longer interparticle distances. The slower dissolution of large particles and the need for long-distance diffusion of carbon poses greater demands on austenitizing prior to quenching (temperature/time). It is an economic disadvantage. The benefit of CGP (soft annealing) is better machinability. On the other hand, this FGP by ASR brings too. In addition, lower quenching temperature and the potential to achieve better mechanical properties favor fine globular pearlite most suitable initial structure before quenching among pearlitic structures.

4 Conclusion

The behavior of three different pearlitic microstructures during the quenching process and resulting mechanical properties were studied for high-strength spring steel 54SiCr6. The initial microstructures were lamellar pearlite produced by hot rolling, coarse globular pearlite obtained by conventional soft annealing, and fine globular pearlite obtained by the process Accelerated Spheroidization and Refinement. Then it was quenched and tempered.

- The lamellar pearlite dissolving during austenitization was very fast. The quenching temperature of 830 °C was sufficient. It achieved the highest yield and ultimate strength but the lowest plastic properties.
- The coarse globular pearlite was slowly dissolved. Therefore it needs higher quenching temperatures. The strain characteristics are lower compared to other microstructures but it had good elongation.
- The dissolution of fine globular pearlite during quenching was similar to lamellar pearlite. The quenching temperature of 830 °C was good. The strength characteristics were almost like in lamellar pearlite but it

achieved excellent elongation and unique reduction of area.

- The hardness measurement was not distinguishing the different initial states after quenching if the ferrite is fully austenitized. The SEM observation found a difference only in coarse globular pearlite, the evolution of quenched structures with lamellar and fine globular pearlite is identical.

Acknowledgement

The result was supported by ERDF Research of advanced steels with unique properties, No. CZ02.1.01/0.0/0.0/16_019/0000836.

References

[1] JANDA, T. (2018). Use of metallographic analysis for evaluating microstructures in quenched and tempered high-strength steel. In: *Manufacturing Technology*, Vol. 18. No.1, pp. 47–52, ISSN 12132489

[2] ESTERL, R., SONNLEITNER, M., WEISSENSTEINER, I., HARTL, K. and SCHNITZER, R. (2019). Influence of quenching conditions on texture and mechanical properties of ultra-high-strength steels. In: *Journal of Materials Science*, Vol. 54, No. 19, pp. 12875–12886, ISSN 15734803

[3] WU, H.Y., HAN, D.X., DU, Y., GAO, X.H. and DU, L.X. (2022). Effect of initial spheroidizing microstructure after quenching and tempering on wear and contact fatigue properties of GCr15 bearing steel. In: *Materials Today Communications*, Vol. 30, ISSN 2352-4928

[4] KIM, K.H., PARK, S.D., KIM, J.H. and BAE, C.M. (2012). Role of spheroidized carbides on the fatigue life of bearing steel. In: *Metals and Materials International*, Vol. 18, No. 6, pp. 917–921, ISSN 20054149

[5] JENÍČEK, Š., OPATOVÁ, K., HAJŠMAN, J. and VOREL, I. (2022). Evolution of Mechanical Properties and Microstructure in Q&P Processed Unconventional Medium-Carbon Silicon Steel and Comparison between Q&P Processing, Quenching and Tempering, and Austemperingfor. In: *Manufacturing Technology*, Vol. 22, No. 2, pp. 146–155, ISSN 12132489

[6] MAJI, S., SUBHANI, A.R., SHOW, B.K. and MAITY, J. (2017). Effect of Cooling Rate on Microstructure and Mechanical Properties of Eutectoid Steel Under Cyclic Heat Treatment. In: *Journal of Materials Engineering and Performance*, Vol. 26, No. 7, pp. 3058–3070, ISSN 15441024

[7] HARISHA, S.R., SHARMA, S., KINI, U.A. and GOWRI SHANKAR, M.C. (2018). Study on Spheroidization and Related Heat Treatments of Medium Carbon Alloy Steels. In: *MATEC Web of Conferences*, Vol. 144, pp. 1–10, ISSN 2261236X

[8] PANDIT, A.S. and BHADESHIA, H.K.D.H. (2011). Diffusion-controlled growth of pearlite in ternary steels. In: *Proceedings of the Royal Society A: Mathematical, Physical and Engineering Sciences*, Vol. 467, No. 2134, pp. 2948–2961, ISSN 14712946

[9] SALVETR, P., NOVÝ, Z., GOKHMAN, A., KOTOUS, J., ZMEKO, J., MOTYČKA, P. and DLOUHÝ, J. (2020). Influence of Si and Cu Content on Tempering and Properties of 54SiCr6 Steel. In: *Manufacturing Technology*, Vol. 20, No. 4, pp. 516–520, ISSN 12132489

[10] MESQUITA, R.A., BARBOSA, C.A., MORALES, E. V. and KESTENBACH, H.J. (2011). Effect of silicon on carbide precipitation after tempering of H11 hot work steels. In: *Metallurgical and Materials Transactions A: Physical Metallurgy and Materials Science*, Vol. 42, No. 2, p. 461–472, ISSN 10735623

[11] SAHA, A., MONDAL, D.K. and MAITY, J. (2011). An alternate approach to accelerated spheroidization in steel by cyclic annealing. In: *Journal of Materials Engineering and Performance*, Vol. 20, No. 1, pp. 114–119, ISSN 10599495

[12] MAITY, J., SAHA, A., MONDAL, D.K. and BISWAS, K. (2013). Mechanism of accelerated spheroidization of steel during cyclic heat treatment around the upper critical temperature. In: *Philosophical Magazine Letters*, Vol. 93, No. 4, pp. 231–237, ISSN 09500839

[13] VERHOEVEN, J.D. and GIBSON, E.D. (1998). The divorced eutectoid transformation in steel. In: *Metallurgical and Materials Transactions A: Physical Metallurgy and Materials Science*, Vol. 29, No. 4, pp. 1181–1189, ISSN 10735623

[14] TIAN, Y.L. and KRAFT, R.W. (1987). Mechanisms of Pearlite Spheroidization. In: *Metallurgical Transactions*, Vol. 18A, pp. 1403–1414

[15] HAUSEROVÁ, D., DLOUHÝ, J. and KOTOUS, J. (2017). Structure Refinement of Spring Steel 51CrV4 after Accelerated Spheroidisation. In: *Archives of Metallurgy and Materials*, Vol. 62, No. 3, pp. 1473–1477, ISSN 17333490

[16] DLOUHY, J., HAUSEROVA, D. and NOVY, Z. (2016). Influence of the carbide-particle spheroidisation process on the microstructure after the quenching and annealing of 100CrMnSi6-4 bearing steel. In: *Materiali in Tehnologije*, Vol. 50, No. 1, pp. 159–162, ISSN 15803414

[17] JIRKOVA, H., HAUSEROVA, D., KUCEROVA, L. and MASEK, B. (2013). Energy- and time-saving low-temperature thermomechanical treatment of low-carbon plain steel. In: *Materiali in Tehnologije*, Vol. 47, No. 3, pp. 335–339, ISSN 15802949

[18] DLOUHY, J., HAUSEROVA, D. and NOVY, Z. (2015). Carbide morphology and ferrite grain size after accelerated carbide spheroidisation and refinement (ASR) of C45 steel. In: *Materiali in Tehnologije*, Vol. 49, No. 4, pp. 625–628, ISSN 15803414

[19] HAUSEROVA, D., DLOUHY, J. and KOVER, M. (2017). Pearlitic Lamellae Spheroidisation During Austenitization and Subsequent Temperature Hold. In: *Archives of Metallurgy and Materials*, Vol. 62, No. 1, pp. 201–204, ISSN 17333490

[20] BHADESHIA, H.K.D.H. (2012). Steels for bearings. In: *Progress in Materials Science*, Vol. 57, No. 2, pp. 268-435, ISSN 00796425

[21] Úřad pro technickou normalizaci, metrologii a státní zkušebnictví (2018). ČSN EN ISO 6507-1. Kovové materiály - Zkouška tvrdosti podle Vickerse - Část 1: Zkušební metoda. Praha, pp. 1-32, Třídicí znak 42 0374

[22] Úřad pro technickou normalizaci, metrologii a státní zkušebnictví (2021). ČSN EN ISO 6892-1. Kovové materiály - Zkoušení tahem - Část 1: Zkušební metoda za pokojové teploty. Praha, pp. 1-76, Třídicí znak 42 0310